Contents lists available at http://qu.edu.iq

Al-Qadisiyah Journal for Engineering Sciences

Journal homepage: https://qjes.qu.edu.iq

Experimental and theoretical analysis of photovoltaic thermal collector performance with multi-flow channel

Mohammed A. Majeed* and Salah M. Salih

Mechanical Engineering Techniques of Power, Engineering Technical College of Al-Najaf, Al-Furat Al-Awsat Technical University, Al-Najaf, Iraq.

ARTICLE INFO

Article history:
Received 00 January 0000
Received in revised form 00 February 0000
Accepted 00 May 0000

Keywords:
Collector
Electrical
Multi-flow
Photovoltaic
Solar flux
Thermal.

ABSTRACT

A steady-state effect analysis of enhancing the cooling performance of a photovoltaic/thermal (PV/T) collector using a damper that changes the flow direction with the multi-flow channel is investigated numerically and experimentally. The study aims to improve the electrical efficiency of PV/T systems with turbulent generation to increase exchange between absorbent panels and airflow with less pressure drop. The effect of different mass flux rates (MFR) of (0.04, 0.05, 0.06, 0.07, and 0.08) kg/s, and various solar flux of (600, 800, and 1000)W/m^2 on solar cell (PV) temperature and PV/T system performance is studied under indoor test conditions. The results indicated that the air temperature is inversely proportional to the air MFR, and the overall efficiency highly depends on the air MFR and solar flux intensity. In addition, the experiment result shows that the higher value at air MFR (0.04-0.08)kg/s, solar flux (1000 W/m^2) for electrical, thermal, and overall efficiency are (17.03%, 74.14%, and 90.4%), respectively. Moreover, The percentage output power its (28.44%) by (15.93) W leads to pioneering results compared to previous studies

1. Introduction

Promising forecasts reflect the amazing technological advance made possible by using renewable energy sources, delivering immeasurable environmental benefits due to lower harmful emissions than fossil fuels. Through their limitless sources, sustainable energy applications have been recognized and developed. Solar energy is one of the Middle East's most important and abundant sources. It is a form of thermal energy engineering; incoming solar radiation can be concentrated, collected and used in various ways, such as energy generation, solar heaters, and building heating [1]–[5]. Many developing nations have pledged to switch to renewable power sources. Electricity and heat can be generated from the sun using photovoltaic (PV) modules and thermal systems. There are numerous experimental and theoretical investigations on PV/T collectors in the literature. L. Awda, Y. KHALAF, and S. Salih [6] confirmed that with every one-degree increase in solar cell temperature, PV module efficiency reduces by 0.45%. M. A. Hasan and S. K. Parida [7] showed that they used research techniques to investigate the behavior and properties of PV/T systems in simulated surroundings, and a mathematical model will aid in the design of energy generation from the PV/T system, either electrical or thermal, under changing environmental circumstances. A. Fudholi, et al, [8] presented a theoretical analysis to test the performance of a PV/T system with a groove. It was conducted under solar radiation (385 - 820) W/$\boldsymbol{m^2}$, with a (MFR) of (0.007-0.07) kg/s, and the theoretical and experimental findings are in agreement. Sumit Tiwari, et al, [9] found that for a PV/T air collector operating at an (MFR) of 0.01 kg/s, average thermal efficiency, electrical efficiency, and overall thermal efficiency average out to 26.68%,

* *Corresponding author.*
E-mail address: muhammed.ms.etcn16@student.atu.edu.iq (*Mohammed A. Majeed*)

https://doi.org/10.30772/qjes.2024.145157.1057

Nomenclature

A	area (m^2)	α	absorption coefficient
Cp	specific heat of the air (J/kg K)	μ	dynamic viscosity
G	solar flux (W/m^2)	η	efficiency
h	heat transfer coefficient (W/m^2 K)	Ø	any of the variables to be solved
H	collector height (mm)	*Subscripts*	
k	thermal conductivity (W/m K)	*a*	ambient
L	length of a collector (mm)	b	backplate
$\dot{m}$	mass flow rate (kg/s)	c	collector
Re	Reynolds number	f	fluid
Pr	Prandtl number	i	inlet
W	width of a collector (mm)	o	outlet
T	temperature (°C)	pv	photovoltaic
Ub	collector back loss coefficient (W/m^2 K)	r	radiative
Ut	collector top loss coefficient (W/m^2 K)	s	sky
Greek symbols		w	wind
ε	emissivity	*Qm*	thermal energy of multi-channel(W)
σ	Stefan-Boltzmann constant	N	number of a glass cover
τ	Transmission coefficient	l	thickness (mm)

11.26%, and 56.30 %, respectively. Amanlou et al, [10] demonstrated that using sidewalls will give the absorber plate the best air dispersion. The outcome showed a 22.4% increase in total efficiency for air mass flux between 0.008 and 0.016 kg/s. Abuska et al, [11] concentrated that having the conical springs inside the air channel improves the collector's thermal efficiency by 15%. A. M. Alsayah, et al, [12] conducted a theoretical investigation of the performance of solar cells using forced airflow at the cell's base. To select the optimal model to manufacture, the study used numerical simulation software (ANSYS-cfx). J. Kim and Y. Nam, [13] studied a simulation model (CFD) to analyze the cooling path using the fin technique attached to the PV module back. Furthermore, The airflow at the lowest of the PV module was analyzed by making slits in the frame. A. M. Elbreki, et al, [14] investigated the height of the coiled fins, the number of fins, and the fin spacing. CFD was used to investigate wind speed and solar radiation on the performance of a PV module. To perform numerical calculations, the 3D Navier-Stokes energy equations are solved using ANSYS FLUENT. Yan zhao et al, [15] showed that numerical modeling and experimental analysis of a newly designed solar PV/T system, added to it an aluminum structure shaped like a beehive, experimentally, the system was tested at irradiance (200-600) W/m². Ismail Baklouti and Zied Driss [16] improved the thermal/ electrical efficiency of the PV/T system by concentrating the (MFR) and air duct depth of the cooling system. Khelifa et al, [17] They studied presented a computational evaluation of a solar collector called photovoltaic thermal PV/T bi-fluid, which utilizes two separate cooling systems - water and air - to enhance its performance in three dimensions. Touti, Ezzeddine et al, [18] conducted Experimental tests to assess the designed model's impact on the PV/T efficiency. The main objective of this study is to identify the optimal design by employing COMSOL Multiphysics and subsequently evaluating it through experimental testing. Ishak, Muhammad Amir Aziat Bin et al, [19] Investigated the exergy efficiency of a bifacial PV/T solar collector; the results showed that the maximum PV exergy achieved was 47.2W when under solar irradiation of 900W/$\boldsymbol{m^2}$ and a mass flow rate of 0.14 kg/s.

Nazri, Nurul Syakirah et al, [20] suggested a new hybrid system, referred to as photovoltaic/thermal–thermoelectric (PV/T-TE), has been to improve the conversion efficiency of photovoltaic (PV) cells by integrating an intelligent thermal component. Noori Merzah, Basil et al, [21] applied a heat pipe system to improve the performance of the flat solar collector; numerical results showed the optimal volumetric flow rate of cooling fluid in the condenser leads to the collector efficiency. Marwa M. Majeed et al, [22] carried out A study was conducted on an evacuated tube solar collector, incorporating a cylindrical finned heat pipe to increase the contact area between the air and the fin surface. The study involved both experimental and computational methods. Q. Yu, S. Chan et al, [23] they devised and manufactured a revolutionary design of PV/T vacuum collector, which preserves the top and lower absorber space in a vacuum state without additional glass cover causing energy loss. Generally, there is a gap according to the studies published about multi-flow PV/T air collectors.That use air as a heat transfer medium instead of other fluids, due to it is not exposed to the risks of electrical conduction leakage, and its natural abundance. This paper presents a technology that has been used for PV module cooling system design based on this principle of vertical, and horizontal flow.

2. Experimental Setup and Procedures

The first component of the system is the PV panel that needs to be installed initially. The channels that are put on the PV module underside are the second component that uses a damper that changes the flow direction and directs air toward the base of the PV module. The other component is the fan that draws air from under the base to the outside at the end of the duct. The entire system was installed, and all the necessary devices were under the indoor testing condition, as shown in Figures (1), and (2). The multi-

channel is a rectangular channel based on the dimensions of the solar panel, width (W) (0.61 m), height (H) (0.061 m), the aspect ratio (W/H) is set at (10) to achieve a fully turbulent flow in the PV/T collector [24]. It contains several dampers spaced at equal distances (100 mm) interspersed with holes equal to the distance between them, and it consists of channels by number (9) that allow the largest heat exchange process between the air and the back of the PV module. Moreover, small holes (20 mm) wide were made on the other side of the partitions adjacent to the thermal insulator; their purpose is to reduce global warming inside the collector and slow down the air speed where the flow is multiple i.e., in three directions.

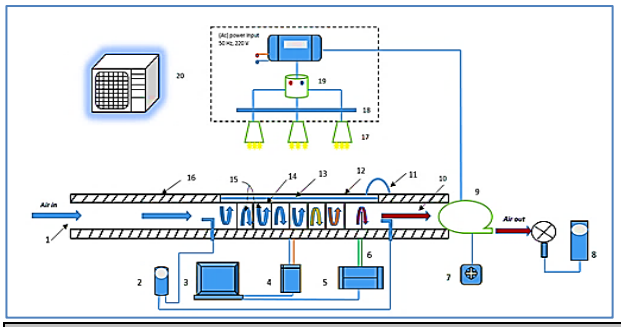

NO.	ITEM	NO.	ITEM
1	Inlet duct	11	Solar Power Meter
2	Pressure manometer	12	Glass layer
3	Laptop	13	PV layer
4	PV analyzer	14	Tadler layer
5	Data Logger	15	Multi-channel
6	Thermocouples Sensor	16	Insulation
7	Velocity regulator	17	Halogen lamps (1000)W
8	Anemometer	18	Electrical connector
9	Air fan(24W)	19	Electrical protection device
10	Outlet duct	20	Air conditioner

Figure. 1 Schematic of the experimental setup.

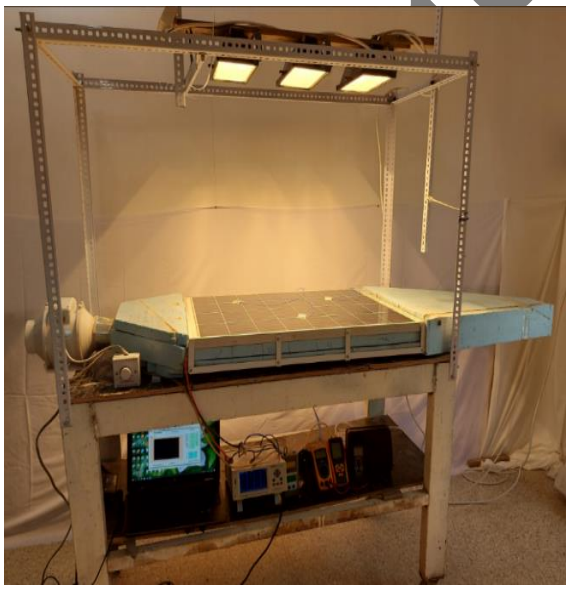

Figure. 2 Photograph of the experimental working setup.

The channels are made of light aluminum with a thickness of (1mm) a length of (860 mm), a width of (610 mm), and a height of (61) mm; these channels were installed with a heat sink on the back of the PV panel to increase thermal conductivity, and thermal insulating (compressed foam) was placed around the air duct on all sides except for the side adjacent to the back of the PV module with a thickness of (30) mm to prevent heat transfer from the surrounding environment into the duct. Furthermore, the length of the air intake duct is (964.4)mm and the length of the outlet air duct is (482.2) mm, according to equations ($5\sqrt{wH}$, $2.5\sqrt{wH}$), respectively [24]. Additionally, a heat sink was used between the surface of the channels and the base of the PV panel to enhance the thermal conductivity, to stop air leakage from the duct silicone was used to seal the gaps between the duct's edge and base before it was screwed into place. Was demonstrated a quality of conductivity through experimental results based on with a notable rise of 22.4% when the air mass flux ranged from and solar flux.

3.Mathematical Modeling

After identifying the following assumptions: The system is under steady-state conditions, Incompressible and turbulent flow, regularity in heat flux, the energy losses from the bottom and wall sides of the PV/T collector to the surrounding are neglected, the useful heat increase is constant along the PV/T air collector and Three-dimensional flow. The physical model of a multi-channel PV/T air collector is described as a system that improves heat transfer and performance PV module.

In this research, the air was recorded temperature values, ambient, PV, inlet, outlet, and solar cell. Major design parameters are given as L= 0.92 m, W= 0.61 m, H= 0.061 m, αg= 0.9, αpv= 0.95, τ = 0.92, εg=0.5, Ta=38°C, Ti = 38°C, and Vw =1 m/s, ηr = 20.66% . The design is illustrated in Figure (3)

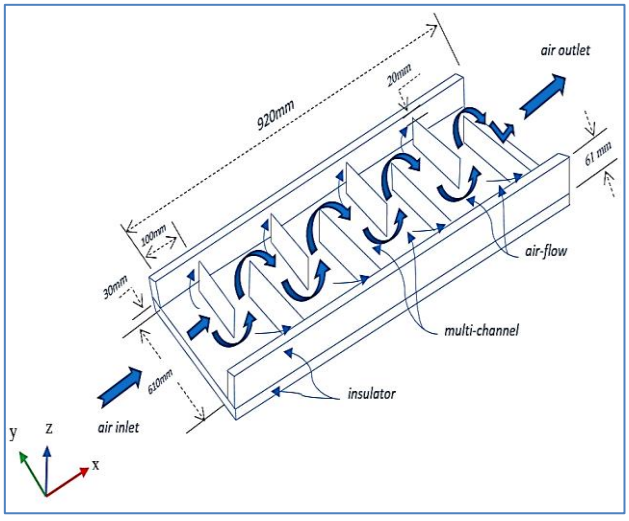

Figure. 3 Schematic illustrating the multi-flow air duct design of the PV/T collector.

3.1 Governing Equations

According to the above assumptions, the temperature distribution of the three-dimensional flow inside the PV/T air collector was governed by the conservation equations(continuity, momentum, and energy) These equations can be written as follows [25]

Continuity equation:

$$\frac{\partial u}{\partial x}+\frac{\partial v}{\partial y}+\frac{\partial w}{\partial z}=0 \quad (1)$$

Momentum equation:

$$\rho\frac{DV}{Dt}=-\nabla P+\rho g=0 \quad (2)$$

Energy equation:

$$\rho\frac{\partial}{\partial xi}(uiT)=\frac{\partial}{\partial xj}\left[(\Gamma+\Gamma t)\frac{\partial T}{\partial xj}\right] \quad (3)$$

The following equations produce the (Γ) molecular thermal diffusivity and (Γt) turbulent thermal diffusivity:

$$\Gamma=\frac{\mu}{pr} \quad (4)$$

$$\Gamma t=\frac{\mu t}{prt} \quad (5)$$

The computation of the turbulent viscosity parameter μt is to be derived from a suitable turbulence model. The equation representing the turbulent viscosity is provided (*k-ε*).

$$\mu t=\rho c\mu\frac{k^2}{\varepsilon} \quad (6)$$

3.2 Boundary Condition fluid part

It is necessary to solve the equations to find the temperature for all surfaces of the PV/T collector, starting from the heat flow at the top surface corresponding to the thermal conductivity throughout the panel and convective heat escape to conductivity at convection on the back surface, ending with the multi-channel cooling system under of the PV panel, bellow illustrates the boundary conditions of the PV/T collector.

$$\begin{cases} At\ x=0 \\ 0<y<w \\ 0<z<H \end{cases} \} T=T\ in \quad \rightarrow \quad u=u\ in$$

$$\begin{cases} At\ x=L \\ 0<y<w \\ 0<z<H \end{cases} \} \frac{\partial \emptyset}{\partial x}=0,$$ where; *∅: is referred to the independent variables of: u;w; v; k ; and ε.*

3.3 Boundary (solid parts)

Figure (4) shows a cross-section of a PV/T collector with multi-flow rectangular channels with different heat transfer coefficients, which can write mathematical equations according.

The steady-state energy balance equations for a PV/T [26]–[28]

For the PV layer:

$$\tau\alpha G=Ut(Tpv-Ta)+h1(Tpv-Tf)+hrpvb(Tpv-Tpvb)+\eta pvG+Qm \quad (7)$$

For airflow channel:

$$\dot{m}Cp(To-Ti)=h1(Tpv-Tf)+h2(Tb-Tf)+Qm \quad (8)$$

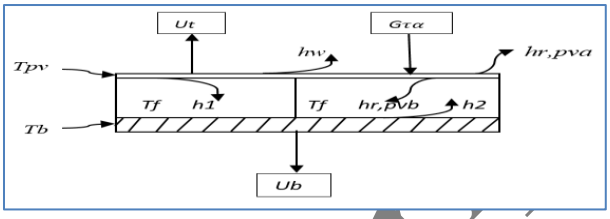

Figure. 4 Heat transfer characteristics of multi-flow rectangular duct in a PV/T air collector schematically.

For back plate:

$$hrpvb(Tpv-Tb)=h2(Tb-Tf)+Ub\,(Tb-Ta) \quad (9)$$

Where:

$$Qm=N.Am.\eta m \quad (10)$$

$$\eta m=\frac{tanMH}{MH} \quad (11)$$

$$M=\left[\frac{2hcl}{kw}\right]^{0.5} \quad (12)$$

$$Ub=[kt/lt] \quad (13)$$

$$Ut=\left[\frac{1}{(hrpa+hw)}\right]^{-1} \quad (14)$$

Characteristics of the air used in a PV/T system, such as viscosity, density, specific heat, and thermal conductivity are constant.

Mean air temperature [29]:

$$\bar{T}f=\frac{(\mathrm{Ti+TO})}{2} \quad (15)$$

The radiation heat transfer coefficient (*hr,pva*) from the glass cover to the ambient is calculated as [27]:

$$hr,pva=\sigma\varepsilon g\frac{(Tg+Tsky)(T^2g+T^2sky)(Tg-Tsky)}{(Tg-Tamb)} \quad (16)$$

The radiation heat transfer coefficient(*hr,pvb*) between the inner surfaces of the air channel is the following[27]:

$$hr,pvb=\sigma\frac{(\mathrm{Tbs+Ti})(\mathrm{T^2bs+T^2i})}{\frac{1}{\varepsilon 1}+\frac{1}{\varepsilon 2-1}} \quad (17)$$

Sky temperature [27] [30]:

$$TsKy=Ta-6 \quad (18)$$

Where *εp*, *σ*, *Ta*, *Tsky*, and *Tpv* are the emissivity of PV, Stefan Boltzman constant, ambient, sky, and PV temperature, respectively.

The convective heat transfer coefficient from glass cover to ambient [27]:

$$hw=2.8+3Vw \quad (19)$$

Where: *h1=h2=h*

The convection heat transfer coefficient (h) and other parameters are calculated using the following formulas[29]:

Convective heat transfer coefficients:

$$h = \frac{k}{D_h} Nu \quad (20)$$

Hydrodynamic channel diameter:

$$D_h = \frac{4wH}{2(w+H)} \quad (21)$$

The Nusselt number (*Nu)* is given by the following formulas (for turbulent flow)

$$Nu = 0.018 Re^{0.8} pr^{0.4} \quad (22)$$

Re and *Pr* are the Reynolds and Prandtl numbers given as:

$$Re = \frac{\dot{m} D_h}{A_{ch} \mu} \quad (23)$$

$$Pr = \frac{\mu cp}{k} \quad (24)$$

The useful energy rate and thermal efficiency can be calculated as follows [27]:

The useful energy rate:

$$Qu = \dot{m} Cp \ (Tfo - fi) \quad (25)$$

The thermal efficiency system [27]:

$$\eta th = \frac{Qu}{GA} \quad (26)$$

The electrical efficiency (*ηpv)* of the PVT air system can be calculated as [31]:

$$\eta pv = \eta r \, [1 - 0.0045(Tpv - 25)] \quad (27)$$

The overall efficiency of the PV/T air system is calculated [8][31]:

$$\eta ov = \eta th + \eta pv \quad (28)$$

4. Grid Independence analysis

In conducting any simulation or analysis, the network architecture must be considered to select the appropriate type, quantity, and location of mesh faces. If the appropriate grid is used, partial differential equations can be solved. Depending on the geometrical form of the project or the operational situation, coarse or fine mesh faces may be used. The grid independence test was used in this simulation to determine the appropriate face size of the mesh. The PV/T system has dimensions of (860×610× 61) mm in length, width, and height, respectively. The mass flow rate (0.08)kg/s and inlet temperature (38)°C at (1000)W/m^2 of solar flux. The average temperature of the fluid that went through the PV/T system was plotted using all grid faces. Figure (5, a) illustrates the grid face count as a function of the PV module outlet temperature. According to the graph below, the best grid has (8,623,938) size. Indeed, more results provide better mesh size accuracy, but increasing the number of meshes lengthens the processing time. Figure (5, b) shows mesh grid faces.

5. Error Analysis

Our present work was done on the experimental and theoretical processes. To confirm the validity of the numerical results against the practical results, we calculate the error percentage between them and compare them with previous researchers. Thus, to estimate the error percentage, the following law was used [32]. Errors were also analyzed for the experimental work with the accuracy of the measuring devices, as in Table (1).

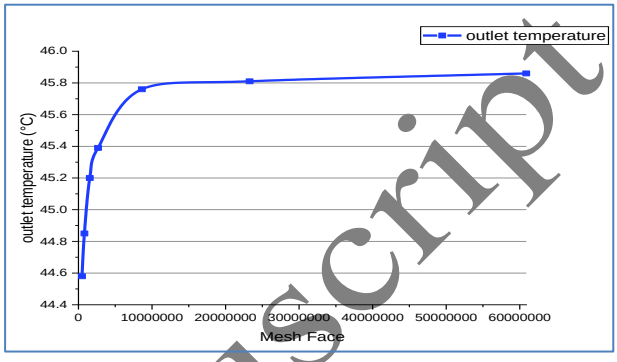

(a)

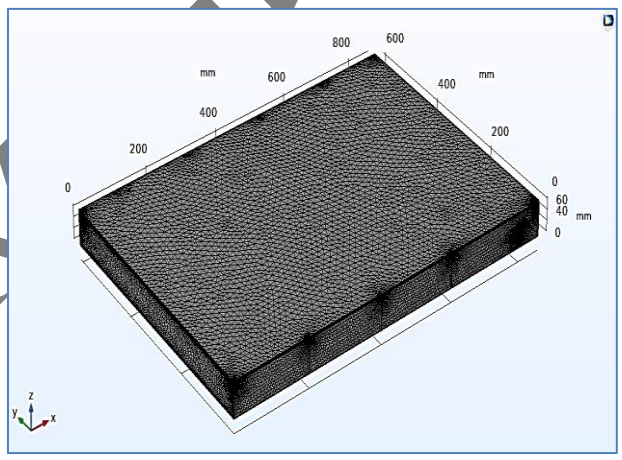

(b)

Figure. 5 The grid independence test of the PV/T system. (a) outlet temperature versus the number of mesh elements. (b) mesh grid faces by COMSOL multiphysics (5.5).

$$Error\ ratio = \frac{NUM-EXP}{NUM} \times 100\% \quad (29)$$

Table. 1 accuracy for the measuring instruments

Instruments	Accuracy	Range
Solar power meter	± 10 W/m^2	0 .1– 1999 W/m^2
Anemometer	± 0.2 m/s	0 – 32.4 m/s
Thermocouples	± 1.2 ºC	0– 1200 ºC

6. Results and Discussion

A mathematical model (theoretical) for predicting the performance of the PV/T air system by multi-flow channel gives good results in reducing the temperature of the solar cells and thus enhancing their performance and

efficiency. The simulations were performed under conditions similar to the experimental method at three solar fluxes levels (600, 800, and 1000) W/m^2, respectively. Each level has five of MFR (0.04, 0.05, 0.06, 0.07, and 0.08) kg/s.

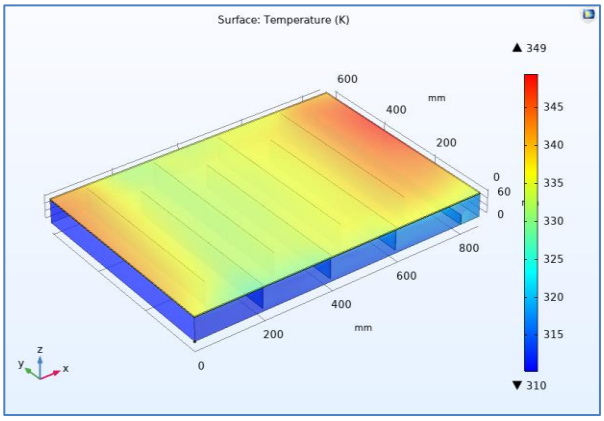

(a)

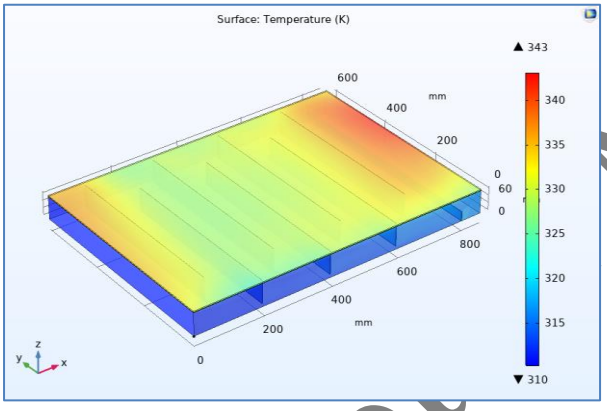

(b)

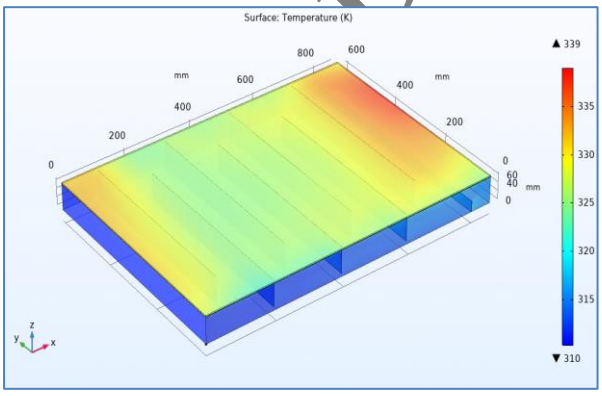

(c)

Figure. 6 Isotherm of the PV/T system with multi-flow channel at solar flux 1000 W/m^2, with different speeds. (a) 2m/s, (b) 3m/s, and (c) 4m/s.

The results indicated a progressive decrease in the temperature of the PV. The use of airflow cooling has been observed to effectively decrease the temperature of solar cells, thereby leading to an improvement in their overall performance and efficiency. The simulations were conducted using conditions that were similar to the experimental approach used for a PV/T collector with a multi-flow channel

During a numerical study of the PV/T system by mass flux inside the thermal collector, the ambient temperature fixed at (38) °C and the inlet flow air temperature fixed at (38)°C. Figure (6. a, b,and c) shows the temperature distribution of the PV/T system. The results found that the temperature profile of the PV surface reduced along the collector, gradually. Increasing the speed of airflow leads to a reduction in the temperature of the solar cells and thus enhances their performance and efficiency, Moreover.Various results for the solar cell temperature and the outlet temperature , as well as changes in electrical efficiency and thermal efficiency, were obtained. As illustrated in Figures (7 - 10), respectively. Figures (7) and (8) showed a decrease in cell temperature and outlet air temperature with increasing air mass flux at different solar flux rates, respectively. at (600 W/m^2) a cell temperature from (56.8-50.6)°C, at (1000 W/m^2) a cell temperature from (64.7-56.1)°C, at (600 W/m^2) a outlet temperature from (42.3-40.2)°C, and at (1000 W/m^2) a outlet temperature from (46.5-42.8)°C. Figures (9) and (10) showed an increase in electrical and thermal efficiencies under the same conditions, respectively, at (600 W/m^2) an electrical efficiency from (17.3-17.86)%, at (1000 W/m^2) an electrical efficiency from (16.3-17.35)%, at (600 W/m^2) a thermal efficiency from (61.2-70.3)°C, and at (1000 W/m^2) a thermal efficiency from (65.9-75)°C.

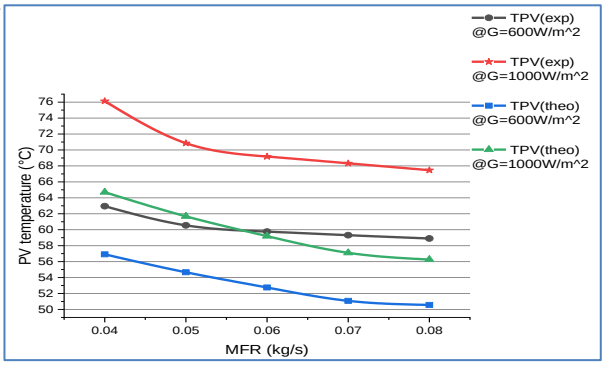

Figure. 7 Theoretical and experimental results for PV temperature versus MFR under solar fluxes (600, and 1000) W/m^2.

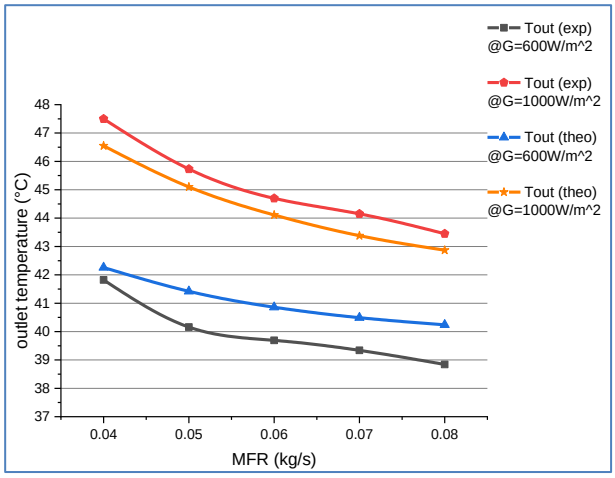

Figure. 8 Theoretical and experimental results for (Tout) versus MFR under solar fluxes (600, and 1000) W/m^2.

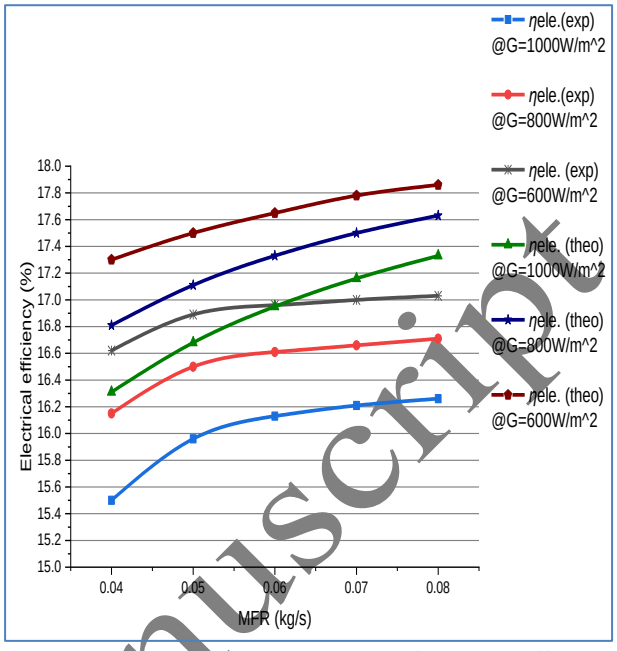

Figure. 9 Theoretical and experimental results for electrical efficiency of the PV/T air collector under different solar fluxes.

Experimentally, the heat from the PV panel is absorbed by the air passing under the PV panel through the multi-flow channels in the thermal collector and thus will influence the cooling of the PV panel unevenly due to the variation in the MFR in the multi-flow channel air collector and can be seen, according to an MFR of (0.04 - 0.08) kg/s, which was applied with solar flux for the internal test conditions, at (600, 800, and 1000) W/m^2. The results exhibited that by increasing the mass flux at any solar flux level, the temperature of the PV/T system and the outside air decreases as well and the solar cell temperature reduces due to the rise in heat exchange between the heat transfer medium and the PV panel, this approach is readily visible. For the PV/T system with a mass flux of (0.04-0.08) kg/s, with a solar flux of (600) W/m^2, the cell temperature decreased from (62.95)°C to (58.9)°C, as shown in Figure (7). Figure (8) The outlet temperature(Tout) decreases from (41.82) °C to (38.84) °C and at the same time, the electrical efficiency increases from (16.62) % to (17.03) % as shown in Figure (9). In addition, the thermal efficiency increased from (53.49) % to (65.57) % as shown in Figure (10). When the solar flux increased to (1000) W/m^2, for the same mass flux, The cell temperature decreased from (76.13)°C to (67.47)°C as shown in Figure (7), Furthermore, the outlet temperature(Tout) decreased from (47.5) °C to (43.45)°C, as illustrated in Figure (8), the electrical efficiency improved from (15.5)% to (16.26)% as illustrated in Figure (9), and the thermal efficiency increased from (64.63)% to (74.14)% as shown in Figure (10).

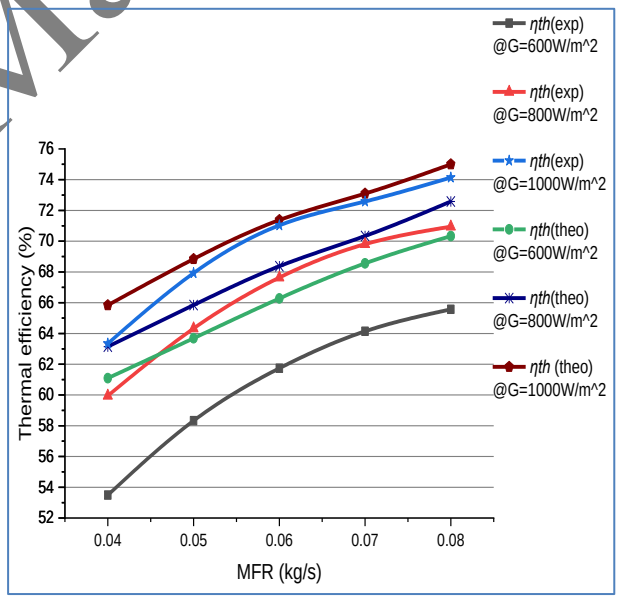

Figure. 10 Theoretical and experimental results for thermal efficiency of the PV/T air collector under different solar fluxes.

Furthermore, recorded experimental results for overall efficiency increased range at a solar flux (600, and 1000)W/m^2 are (70.11-82.6)%, (78.84-90.4)%, respectively. As shown in Figure (11). In addition, theoretical results showed that at a solar flux (600, and 1000)W/m^2 are (78.39 - 88.19)%, (82.15 - 92.33)%, respectively. As shown in Figure (12)

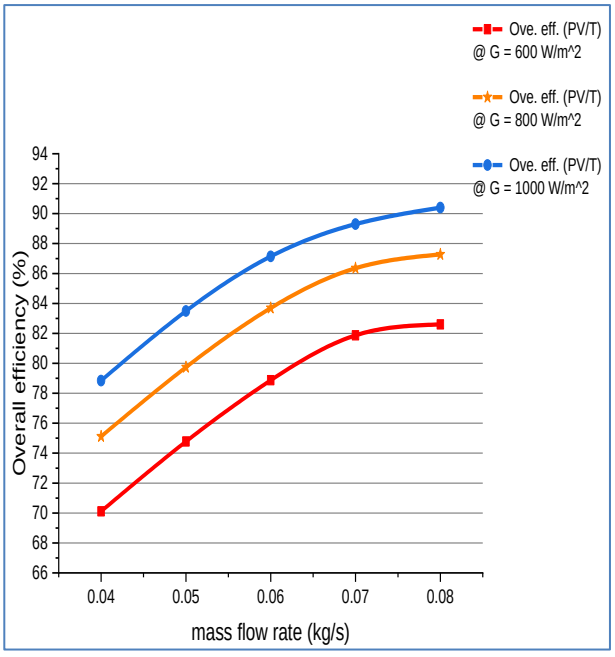

Figure. 11 Experimental illustrations of the relation between MFR and overall efficiency, at different rates of solar fluxes.

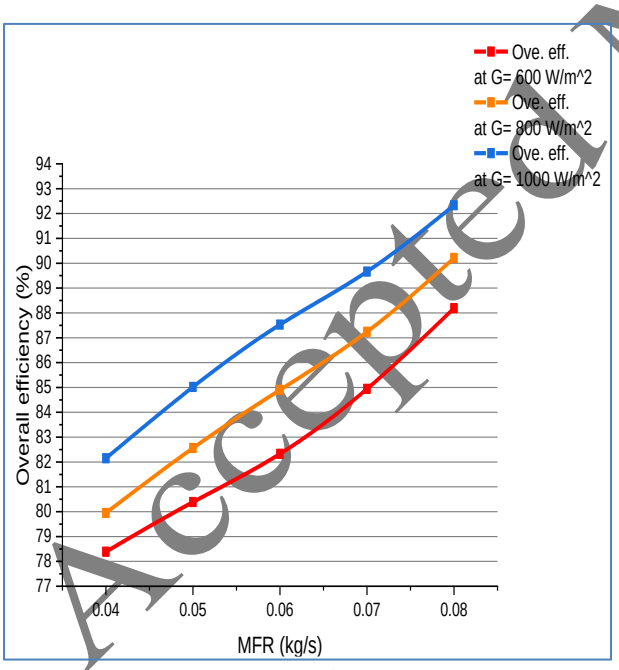

Figure 12 Theoretical illustrations of the relation between MFR and overall efficiency under different rates of solar fluxes.

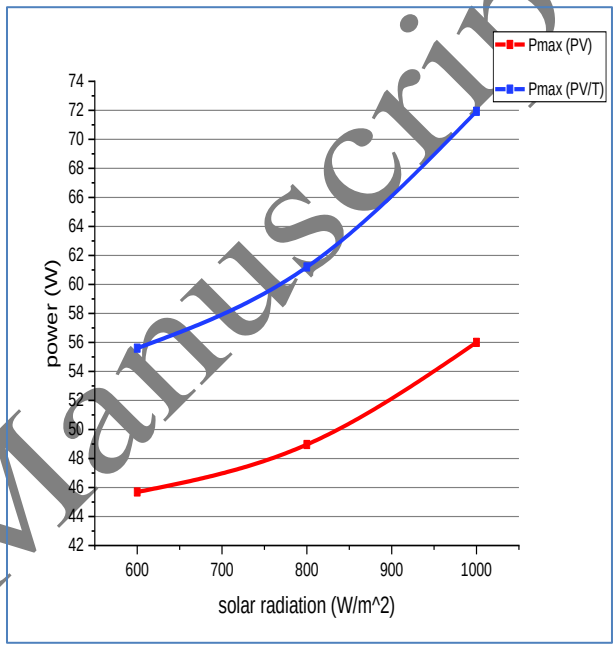

Figure. 13 Comparison of the PV/T air system at MFR of (0.08) kg

Figure 13 clearly shows the maximum power value (Pmax) of the PV/T system, indicating an obvious rise in power as the solar flux increases in comparison to the traditional PV panel.

Table 2. compares the results present with previous Studie

Author	Solar thermal system	Reduction of the cell temperature (°C)	Percentage increase in cell performance(%)
Rakesh Kumar, Marc A. Rosen [2011], [33]	Double pass solar PV/T air the system with and without fins	16	Increase electrical efficiency 4.8
. Mazón-Hernández et al, [2013], [34]	Improving PV panel electrical performance with generated or forced airflow	15	Increase in output power 15
Hussein M. Maghrabie et al, [2017], [35]	Improvement of PV cell performance by active air cooling system	5	Increase in output power 4.4
Fudholi Ahmad et al [2017], [8]	Analyses of the energy and exergy of the PV/T combination with ∇-groove	More than 25	Increase electrical efficiency by more than 2.7
Haidar Zeyad A Orfi et al, [2018], [36]	Experimental investigation of evaporative cooling to enhance the efficiency of PV panels	More than 20	Increase in output power 10-14
Mohsin Ahmed et al, [2019], [37]	New technology (guide air) to cool the PV module with forced air	22.278	Increase in output power 14.88
Ridwone Hossain et al, [2020], [38]	New design of hybrid PV/T system to improve PV cell performance	(Tout- Tin) = More than 4	Increase in output power 5.4
Present study	Enhancement of performance PV/T air system by using multi-flow channels	19.53	Increase in output power 28.44 Increase electrical efficiency 2.52

7. Conclusions

The current work necessitates a comparison with previous studies to ascertain the range of performance enhancement, as illustrated in Table (2). A mathematical model that compares experimental results to predict the performance of a PV/T air collector with a multi-flow channel. The numerical model results agree with the experimental data at an approximate error (1.57). The increased mass flow rate led to a reduction in the PV temperature, and improved electrical performance. Higher electrical and thermal efficiency, experimental and numerical, at a mass flow rate (0.08) kg/s are (17.03, 17.86) %, (74.14, 75) %, respectively. The percentage of the decrease in the PV temperature at the mass flow rate (0.08 kg/s) is (28.94%), and the maximum PV temperature reduction is about (19.53°C). The percentage rise in the maximum power of the PV module after the cooling process its range (28.44) %, by (15.93) W. The overall efficiency maximum of the PV/T air collector with a multi-flow channel recorded with a solar flux rate (1000)W/m^2 , at MFR (0.08) kg/s, for experimental and numerical results are (90.4)%, and (92.33)%, respectively.

Authors' contribution

All authors contributed equally to the preparation of this article.

Declaration of competing interest

The authors declare no conflicts of interest.

Funding source

This study didn't receive any specific funds.

REFERENCES

[1] J.Dominguez,Soteris_A._Kalogirou. Solar_Energy_Engineering._Processes_and_Systems-Academic_Press_2014 with-cover-page-v2.pdf. 2014.

[2] S. M. Salih, J. M. Jalil, and S. E. Najim, "Experimental and numerical analysis of double-pass solar air heater utilizing multiple capsules PCM," Renew. Energy, vol. 143, pp. 1053–1066, 2019, doi: 10.1016/j.renene.2019.05.050

[3] M. I. Hasan and D. Mohammed Muter, "A review of earth to air heat exchanger as a passive cooling and heating technique and the affecting parameters," Al-Qadisiyah J. Eng. Sci., vol. 14, pp. 21–29, 2021, doi: 10.30772/qjes.v14i1.735

[4] M. F. Yousif and M. A. Theeb, "A review of solar air collectors with baffles and porous medium: Types and applications," Al-Qadisiyah J. Eng. Sci., vol. 16, no. 1, pp. 37–41, 2023, doi: 10.30772/qjes.v16i1.841

[5] D. Nadheer Abd zaid and D. A Hamzah, "Heat Transfer Enhancement by Turbulence Generator inside Heat Receiver," Al-Qadisiyah J. Eng. Sci., vol. 13, pp. 268–273, 2020,

[6] L. Awda, Y. KHALAF, and S. Salih, "Analysis of temperature effect on a

crystalline silicon photovoltaic module performance," Int. J. Eng., vol. 29, no. 5, pp. 722–727, 2016, [Online]. Available: https://www.ije.ir/article_72728.html

[7] M. A. Hasan and S. K. Parida, "An overview of solar photovoltaic panel modeling based on analytical and experimental viewpoint," Renew. Sustain. Energy Rev., vol. 60, pp. 75–83, 2016, doi: org/10.1016/j.rser.2016.01.087

[8] A. Fudholi et al., "Energy and exergy analyses of photovoltaic thermal collector with∇-groove," Sol. Energy, vol. 159, no. November 2016, pp. 742–750, 2018, doi: 10.1016/j.solener.2017.11.056

[9] P. Jha, B. Das, and R. Gupta, "An experimental study of a photovoltaic thermal air collector (PVTAC): A comparison of a flat and the wavy collector," Appl. Therm. Eng., vol. 163, no. September, p. 114344, 2019, doi: 10.1016/j.applthermaleng.2019.114344

[10] Y. Amanlou, T. T. Hashjin, B. Ghobadian, and et G. Najafi, "Air cooling low concentrated photovoltaic/thermal (LCPV/T) solar collector to approach uniform temperature distribution on the PV plate," Appl. Therm. Eng., vol. 141, pp. 413–421, 2018, doi: org/10.1016/j.applthermaleng.2018.05.070

[11] M. Abuşka and M. B. Akgül, "Experimental study on thermal performance of a novel solar air collector having conical springs on absorber plate," Arab. J. Sci. Eng., vol. 41, pp. 4509–4516, 2016, doi: org/10.1007/s13369-016-2177-4

[12] A. M. Alsayah, M. H. K. Aboaltabooq, M. H. Majeed, and B. A. S. Bassam Abed, "CFD study to improve PV cell performance by forced air: Modern design," Period. Eng. Nat. Sci., vol. 7, no. 3, pp. 1468–1477, 2019, doi: 10.21533/pen.v7i3.794

[13] J. Kim and Y. Nam, "Study on the cooling effect of attached fins on PV using CFD simulation," Energies, vol. 12, no. 4, 2019, doi: 10.3390/en12040758

[14] A. M. Elbreki, K. Sopian, A. Fazlizan, and A. Ibrahim, "An innovative technique of passive cooling PV module using lapping fins and planner reflector," Case Stud. Therm. Eng., vol. 19, no. January, p. 100607, 2020, doi: 10.1016/j.csite.2020.100607

[15] Y. Zhao, T. Meng, C. Jing, J. Hu, and S. Qian, "Experimental and numerical investigation on thermal performance of PV-driven aluminium honeycomb solar air collector," Sol. Energy, vol. 204, no. June 2019, pp. 294–306, 2020, doi: 10.1016/j.solener.2020.04.047

[16] I. Baklouti and Z. Driss, "Numerical and Experimental Study of the Impact of Key Parameters on a PVT Air Collector: Mass Flow Rate and Duct Depth," J. Therm. Sci., vol. 30, no. 5, pp. 1625–1642, 2021, doi: 10.1007/s11630-020-1345-8

[17] A. Khelifa, M. El Hadi Attia, Z. Driss, and A. Muthu Manokar, "Performance enhancement of photovoltaic solar collector using fins and bi-fluid: Thermal efficiency study," Sol. Energy, vol. 263, p. 111987, 2023, doi: org/10.1016/j.solener.2023.111987

[18] E. Touti, M. Masmali, M. Fterich, and H. Chouikhi, "Experimental and numerical study of the PVT design impact on the electrical and thermal performances," Case Stud. Therm. Eng., vol. 43, p. 102732, 2023,

[19] M. A. A. Bin Ishak, A. Ibrahim, A. Fazlizan, M. F. Fauzan, K. Sopian, and A. A. Rahmat, "Exergy performance of a reversed circular flow jet impingement bifacial photovoltaic thermal (PVT) solar collector," Case Stud. Therm. Eng., vol. 49, no. June, p. 103322, 2023, doi: 10.1016/j.csite.2023.103322

[20] N. S. Nazri et al., "Analytical and experimental study of hybrid photovoltaic–thermal–thermoelectric systems in sustainable energy generation," Case Stud. Therm. Eng., vol. 51, no. June, p. 103522, 2023, doi: 10.1016/j.csite.2023.103522

[21] B. Noori Merzah, M. H. Majeed, and F. A. Saleh, "Numerical study of flat plate solar collector performance with square shape wicked evaporator," Al-Qadisiyah J. Eng. Sci., vol. 12, pp. 90–97, 2019, doi: 10.30772/qjes.v12i2.592

[22] M. M. Majeed and L. M. Nassir, "Statistical analysis of the vacuum solar collector using the analysis of variance method," vol. 16, pp. 273–278, 2023, doi: 10.30772/qjes.2023.180350

[23] Q. Yu, S. Chan, K. Chen, B. Zhao, X. Ren, and G. Pei, "Numerical and experimental study of a novel vacuum Photovoltaic/thermal (PV/T) collector for efficient solar energy harvesting," Appl. Therm. Eng., vol. 236, p. 121580, 2024, doi: org/10.1016/j.applthermaleng.2023.121580

[24] A. Standard, "93-77,'Methods of testing to determine the thermal performance of solar collectors,'" New York, 1977.

[25] R. K. Rajput, A textbook of fluid mechanics and hydraulic machines. S. Chand Publishing, 2004.

[26] A. S. Joshi, A. Tiwari, G. N. Tiwari, I. Dincer, and B. V. Reddy, "Performance evaluation of a hybrid photovoltaic thermal (PV/T) (glass-to-glass) system," Int. J. Therm. Sci., vol. 48, no. 1, pp. 154–164, 2009, doi: 10.1016/j.ijthermalsci.2008.05.001

[27] K. E. Amori and H. M. Taqi Al-Najjar, "Analysis of thermal and electrical performance of a hybrid (PV/T) air based solar collector for Iraq," Appl. Energy, vol. 98, pp. 384–395, 2012, doi: 10.1016/j.apenergy.2012.03.061

[28] A. Fudholi et al., "Exergy and sustainability index of photovoltaic thermal (PVT) air collector: A theoretical and experimental study," Renew. Sustain. Energy Rev., vol. 100, no. July 2018, pp. 44–51, 2019, doi: 10.1016/j.rser.2018.10.019

[29] M. Zohri, S. Hadisaputra, and A. Fudholi, "Exergy and energy analysis of photovoltaic thermal (Pvt)with and without fins collector," ARPN J. Eng. Appl. Sci., vol. 13, no. 3, pp. 803–808, 2018, [Online]. Available: https://scholar.google.com/scholar?q=Exergy+and+energy+analysis+of+photovoltaic+thermal+(Pvt)with+and+without+fins+collector&hl=ar&as_sdt=0&as_vis=1&oi=scholart

[30] A. S. Joshi and A. Tiwari, "Energy and exergy efficiencies of a hybrid photovoltaic-thermal (PV/T) air collector," *Renew. Energy*, vol. 32, no. 13, pp. 2223–2241, 2007, doi: 10.1016/j.renene.2006.11.013

[31] A. Ibrahim, A. Fudholi, K. Sopian, M. Y. Othman, and M. H. Ruslan, "Efficiencies and improvement potential of building integrated photovoltaic thermal (BIPVT) system," *Energy Convers. Manag.*, vol. 77, pp. 527–534, 2014, doi: 10.1016/j.enconman.2013.10.033

[32] Hrvoje Jasak, "Error Analysis and Estimation for the Finite Volume Method with Applications to Fluid Flows," vol. M, no. septembre, p. 200, 1992, [Online]. Available: https://books.google.com.co/books?id=_ghlHAAACAAJ

[33] R. Kumar and M. A. Rosen, "Performance evaluation of a double pass PV/T solar air heater with and without fins," *Appl. Therm. Eng.*, vol. 31, no. 8–9, pp. 1402–1410, 2011, doi: 10.1016/j.applthermaleng.2010.12.037

[34] R. Mazón-Hernández, J. R. García-Cascales, F. Vera-García, A. S. Káiser, and B. Zamora, "Improving the electrical parameters of a photovoltaic panel by means of an induced or forced air stream," *Int. J. Photoenergy*, vol. 2013, 2013, doi: org/10.1155/2013/830968

[35] H. M. Maghrabie, A. S. A. Mohamed, M. S. Ahmed, H. M. Maghrabie, and M. S. Ahmed, "Improving Performance of Photovoltaic Cells via Active Air Cooling System," in *Proc. 4th Int. Conf. Energy Eng*, 2017, pp. 1–5. [Online]. Available: https://scholar.google.com/citations?view_op=view_citation&hl=ar&user=IQkfp4sAAAAJ&citation_for_view=IQkfp4sAAAAJ:eQOLeE2rZwMC

[36] Z. A. Haidar, J. Orfi, and Z. Kaneesamkandi, "Experimental investigation of evaporative cooling for enhancing photovoltaic panels efficiency," *Results Phys.*, vol. 11, pp. 690–697, 2018, doi: org/10.1016/j.rinp.2018.10.016

[37] A. M. Kudhair, "NUMERICAL AND EXPERIMENTAL INVESTIGATION ON IMPROVING PHOTOVOLTAIC MODULE EFFICIENCY USING AIR GUIDE COOLING," no. November 2019, 2012.

[38] R. Hossain *et al.*, "New Design of Solar Photovoltaic and Thermal Hybrid System for Performance Improvement of Solar Photovoltaic," *Int. J. Photoenergy*, vol. 2020, no. 1, 2020, doi: 10.1155/2020/8825489